

$J/\psi + jet$ diffractive production in the direct photon process at HERA

Jia-Sheng Xu

Department of Physics, Peking University, Beijing 100871, China

Hong-An Peng

*China Center of Advance Science and Technology (World Laboratory), Beijing 100080, China
and Department of Physics, Peking University, Beijing 100871, China*

Zhan-Yuan Yan, and Zhen-Min He

Department of Physics, Hebei Teacher's University, Shijiazhuang 050016, China

Abstract

We present a study of $J/\psi + jet$ diffractive production in the direct photon process at HERA based on the factorization theorem for lepton-induced hard diffractive scattering and the factorization formalism of the nonrelativistic QCD (NRQCD) for quarkonia production. Using the diffractive gluon distribution function extracted from HERA data on diffractive deep inelastic scattering and diffractive dijet photon production, we show that this process can be studied at HERA with present integrated luminosity, and can give valuable insights in the color-octet mechanism for heavy quarkonia production.

PACS number(s): 12.40Nn, 13.85.Ni, 14.40.Gx

I. INTRODUCTION

Diffractive scattering was imported into high energy strong interaction to interpret the t distribution of elastic hadron-hadron scattering at small $|t|$ region [1]. In the framework of the Regge theory, diffractive scattering is assumed to take place through the exchange of an object with the quantum numbers of the vacuum (the Pomeron) [2]. Although, the Pomeron plays a particular and very important role in soft processes in hadron-hadron collisions, the true nature of it and its interaction with hadrons remain a mystery.

Due to the nature of color singlet exchange, the diffractive scattering events are characterized by a large rapidity gap, a region in rapidity devoiding of hadronic energy flow. Events containing rapidity gap and jets were first observed by UA8 Collaboration at CERN [3], opening the field of hard diffraction. The hard diffraction is also observed and studied by various experiments [4–8]. Although it is still difficult to understand the soft diffractive scattering in the framework of QCD, much progresses in understanding the nature of hard diffraction are made in the light of great theoretical and experimental efforts [9]. As an attempt of understanding hard diffraction on the parton level, Ingelman and Schlein [10] assumed that the Pomeron, similar to the nucleon, is composed of partons, mainly of gluons, and the hard diffractive processes can probe the partonic structure of the Pomeron. In fact, the Ingelman-Schlein model for hard diffraction is based on the assumption of hard diffractive scattering factorization together with Regge factorization for the Pomeron exchange. But, comparison the total $pp(\bar{p})$ single diffraction cross section data [11] with predictions based on the Regge factorization for the Pomeron exchange indicates the breakdown of the Regge factorization [12]. Furthermore, as pointed by Ingelman in [9], there are conceptual and theoretical problems with the Ingelman-Schlein model. First, the Pomeron is not a real state, it is only a virtual exchanged spacelike object. the concept of a structure function is then not well defined. In fact, the factorization of diffractive structure function into a Pomeron flux and a pomeron structure function cannot be uniquely defined since only the product is an observable quantity. Second, the Pomeron-proton interaction is soft, its space-time scale is larger compared to that of the hard interaction, so the Pomeron can then not be considered as decoupled from the proton, and in particular, is not a separate part of the QCD evolution in the proton.

For the lepton induced hard diffractive scattering processes, such as diffractive deep inelastic scattering (DDIS) and diffractive direct photoproduction of jets, there is indeed a factorization theorem which has been proven by Collins [13] recently. It is the same as factorization for inclusive hard processed, except that parton densities are replaced by diffractive parton densities [14,15]. The diffractive parton densities (the primary non-perturbative quantities in hard diffraction) obey exactly the same DGLAP evolution equations as ordinary parton densities, and have been extracted from HERA data on DDIS and on diffractive photonproduction of jets [16]. This factorization theorem also establishes the universality of the diffractive parton distributions for those processes to which the theorem applies, hence justifies, from fundamental principles, the analysis of ZEUS and H1 Collaboration [6,5] on hard diffraction, provided the term “ Pomeron ” used in these analyses is as a label for a particular kind of parametrization for diffractive parton densities, and an indication of the vacuum quantum numbers to be exchanged. In the light of hard diffractive factorization proven by Collins [13], the Ingelman-Schlein model for hard diffraction assumed further the factorization of diffractive parton densities into a universal Pomeron flux and a Pomeron parton densities, but such further factorization is unjustifiable.

In this paper, we present a study of another hard diffractive process, $J/\psi + jet$ diffractive production in the direct photon process at HERA

$$\gamma(q) + p(p_1) \rightarrow p(p'_1) + J/\psi(P) + jet + X, \quad (1)$$

where q, p_1, p'_1 , and P are the momenta of incoming photon, proton, outgoing proton, and J/ψ respectively. We base on the factorization theorem for lepton-induced hard diffractive scattering and the factorization formalism of the nonrelativistic QCD (NRQCD) for quarkonia production. Using the diffractive gluon distribution function extracted from HERA data on DDIS and diffractive dijet photon production, we show that this process can give valuable insights in the color-octet mechanism for heavy quarkonia production. This process was briefly discussed in [17] where the relativistic corrections to photoproduction of J/ψ were studied in the so-called color-singlet model (CSM) [18].

Our paper is organized as follows. We describe in detail our calculation scheme in Sec.II, in which, a brief introduction of the heavy quarkonium production mechanism, the hard subprocesses for $J/\psi + jet$ production and a summary of the kinematics related to the J/ψ 's z and P_T distributions are included. Our results and discussions are given in Sec. III.

II. CALCULATING SCHEME

Based on the factorization theorem for lepton-induced hard diffractive scattering and the factorization formalism of NRQCD for heavy quarkonia production, $J/\psi + jet$ diffractive production process is shown in Fig.1 . This process consists two steps. First, the almost point-like $c\bar{c}$ pair with large P_T is produced in the hard subprocesses, then J/ψ particle is produced from this point-like $c\bar{c}$ pair via soft interactions.

A. Heavy quarkonium production mechnism

Heavy quarkonium production in various processes has been the focus of much experimental and theoretical attention during the past few years [19]. This is mainly due to the observation of large discrepancies between experiment measurements of prompt and direct J/ψ production and ψ' production at large P_T at the Collider Detector Facility (CDF) at the Fermilab Tevatron and the calculations based on CSM [20].

The first major conceptual advance in heavy quarkonium production was the realization that fragmentation dominates at sufficiently large P_T [21] which indicates that most charmonium at large P_T is produced by the fragmentation of individual large P_T partons. The fragmentation functions are calculated in CSM. Including this fragmentation mechanism indeed brings the theoretical predictions for prompt J/ψ production at the Tevatron to within a factor of 3 of the data [22]. But the prediction for the ψ' production cross section remains a factor of 30 below the data even after including the fragmentation contribution (the ψ' “surplus” problem). Furthermore, the presence of the logarithmic infrared divergences in the production cross sections for P-wave charmonium states and the annihilation rate for $\chi_{cJ} \rightarrow q\bar{q}g$ indicate CSM is incomplete. All these indicate that important production mechanism beyond CSM needs to be included [23] [24]. So the color-octet mechanism [19] is proposed which is based on the factorization formalism of NRQCD [25] [26]. Contrary to the basic assumption of CSM, the heavy quark pair in a color-octet state can make a transition into physical quarkonium state through soft color interactions.

Although the color-octet fragmentation picture of heavy quarkonium production [24] has provided valuable insight, the approximation that enter into fragmentation computations break

down when a quarkonium's energy becomes comparable to its mass. The fragmentation predictions for heavy quarkonium production are therefore unreliable at low P_T . Based upon the above several recently developed ideas in heavy quarkonium physics, Cho and Leibovich [27] identify a large class of color-octet diagrams that mediate quarkonia production at all energies, which reduce to the dominant set of gluon fragmentation graphs in the high P_T limit. By fitting the data on heavy quarkonia production at the Tevatron, numerical values for the long distance matrix elements are extracted [27,28], which are generally consistent with NRQCD power scaling rules [29].

In order to convincingly establish the color-octet mechanism, it is important to test whether the same matrix elements be able to explain heavy quarkonium production in other high energy processes, such as inclusive J/ψ production in e^+e^- annihilation and inelastic J/ψ photoproduction at HERA *et al.* . Other mechanism for heavy quarkonium production can be found in [30,31].

B. The hard subprocesses for $J/\psi + jet$ production

J/ψ is described within the NRQCD framework in terms of Fock state decompositions as

$$\begin{aligned} |J/\psi\rangle = & O(1) |c\bar{c}[{}^3S_1^{(1)}]\rangle + O(v) |c\bar{c}[{}^3P_J^{(8)}]g\rangle \\ & + O(v^2) |c\bar{c}[{}^1S_0^{(8)}]g\rangle + O(v^2) |c\bar{c}[{}^3S_1^{(1,8)}]gg\rangle \\ & + O(v^2) |c\bar{c}[{}^3P_J^{(1,8)}]gg\rangle + \dots, \end{aligned} \quad (2)$$

where the $c\bar{c}$ pairs are indicated within the square brackets in spectroscopic notation. The pairs' color states are indicated by singlet (1) or octet (8) superscripts. The color octet $c\bar{c}$ state can make a transition into a physical J/ψ state by soft chromoelectric dipole (E1) transition(s) or chromomagnetic dipole M1 transition(s)

$$(c\bar{c})[{}^{2S+1}L_J^{(8)}] \rightarrow J/\psi. \quad (3)$$

NRQCD factorization scheme [25] has been established to systematically separate high and low energy scale interactions. It is based upon a double power series expansion in the strong interaction fine structure constant α_s and the small velocity parameter v . The production of a $(c\bar{c})[{}^{2S+1}L_J^{(1,8)}]$ pair with separation less than or of order $\frac{1}{m_c}$ can be calculated perturbatively. The long distance effects for the produced almost point-like $c\bar{c}$ to form the bound state are isolated into nonperturbative matrix elements. Furthermore, NRQCD power counting rules can be exploited to determine the dominant contributions to various quarkonium processes [29]. For direct J/ψ production, the color-octet matrix elements, $\langle 0 | \mathcal{O}_8^{J/\psi} [{}^3S_1] | 0 \rangle$, $\langle 0 | \mathcal{O}_8^{J/\psi} [{}^1S_0] | 0 \rangle$ and $\langle 0 | \mathcal{O}_8^{J/\psi} [{}^3P_J] | 0 \rangle / m_c^2$ are all scaling as $m_c^3 v_c^7$. So these color-octet contributions to J/ψ production must be included for consistency.

On the partonic level, $J/\psi + jet$ production are composed of the photon gluon fusion, which are sketched in Fig.2. These are

$$\begin{aligned} \gamma + g & \rightarrow g + (c\bar{c})[{}^3S_1^{(1)}, {}^3S_1^{(8)}], \text{ Fig.2.(a) - (f);} \\ \gamma + g & \rightarrow g + (c\bar{c})[{}^1S_0^{(8)}, {}^3P_J^{(8)}], \text{ Fig.2.(a) - (h).} \end{aligned}$$

The quark initiated subprocesses ($\gamma q(\bar{q})$ channel) are strongly suppressed and will be neglected further.

The color SU(3) coefficients are given by

$$\langle 3i; \bar{3}j|1\rangle = \delta_{ji}/\sqrt{3}, \quad \langle 3i; \bar{3}j|8a\rangle = \sqrt{2}T_{ji}^a. \quad (4)$$

Some identities involving the traces of the color matrices are useful when the matrix elements are squared and spin, color averaged:

$$\begin{aligned} \frac{1}{8}\text{Tr}(T^b T^c)\text{Tr}^*(T^b T^c) \frac{1}{\sqrt{3}} \frac{1}{\sqrt{3}} &= \frac{1}{12}, \\ \frac{1}{8}F_c^{(a)-(c)}F_c^{*(a)-(c)} &= \frac{7}{12}, \\ \frac{1}{8}F_c^{(a)-(c)}F_c^{*(d)-(f)} &= \frac{-1}{6}, \\ \frac{1}{8}F_c^{(d)-(f)}F_c^{*(a)-(c)} &= \frac{-1}{6}, \\ \frac{1}{8}F_c^{(d)-(f)}F_c^{*(d)-(f)} &= \frac{7}{12}, \\ \frac{1}{8}F_c^{(g)-(h)}F_c^{*(h)-(g)} &= \frac{3}{2}, \\ \frac{1}{8}F_c^{(g)-(h)}F_c^{*(a)-(c)} &= \frac{-3i}{4}, \\ \frac{1}{8}F_c^{(g)-(h)}F_c^{*(d)-(f)} &= \frac{3i}{4}, \\ \frac{1}{8}F_c^{*(g)-(h)}F_c^{(a)-(c)} &= \frac{3i}{4}, \\ \frac{1}{8}F_c^{*(g)-(h)}F_c^{(d)-(f)} &= \frac{-3i}{4}. \end{aligned} \quad (5)$$

Where

$$\begin{aligned} F_c^{(a)-(c)} &= \sqrt{2}\text{Tr}(T^a T^b T^c), \\ F_c^{(d)-(f)} &= \sqrt{2}\text{Tr}(T^a T^c T^b), \\ F_c^{(g)-(h)} &= \sqrt{2}\text{Tr}(T^a T^d) f_{dbc} \\ &= \frac{\sqrt{2}}{2} f_{abc}. \end{aligned} \quad (6)$$

Note that the hard subprocesses that producing color-octet $(c\bar{c})[{}^1S_0^{(8)}, {}^3P_J^{(8)}]$ pair involve triple-gluon coupling (Two of them are external gluons). This situation implies that we cannot use the trick of replacing the sum over gluon polarization states by

$$\sum_{\lambda} \varepsilon_{\alpha}(\lambda) \varepsilon_{\alpha'}^*(\lambda) \rightarrow -g_{\alpha\alpha'}, \quad (7)$$

when we use the Feynman gauge for the gluon propagator [32]. One way to obtain the correct result is insist that the polarization states of the two external gluons are physical (*i.e.*, transverse). This is accomplished by the projection

$$\begin{aligned} &\sum_{\lambda} \varepsilon_{\alpha}(\lambda) \varepsilon_{\alpha'}^*(\lambda) \\ &= -\left[g_{\alpha\alpha'} - \frac{n_{\alpha} k_{\alpha'} + n_{\alpha'} k_{\alpha}}{(n\dot{k})} + \frac{n^2 k_{\alpha} k_{\alpha'}}{(n\dot{k})^2} \right], \end{aligned} \quad (8)$$

where n is an arbitrary 4-vector and k is the gluon 4-momentum. This is analogous to using an axial (*i.e.* physical) gauge for the gluon propagator. Our choice for the 4-vector n is $n = g_2$

for the incoming gluon and $n = g_1$ for the outgoing gluon, g_1, g_2 are the 4-momenta of the incoming and outgoing gluons respectively.

With all ingredients set as above, we obtain the spin, color average-squared matrix elements $\overline{\Sigma}|M(\gamma + g \rightarrow (c\bar{c})[^{2S+1}L_j^{(1;8)}] + g)|^2$. Our analytic expressions are consistent with [33] and the results calculated from Eqs. (11),(15) and appendix B of [34], but different from the expressions of [35]. For example, the expression of $\overline{\Sigma}|M(\gamma + g \rightarrow (c\bar{c})[^1S_0^{(8)}] + g)|^2$ of [35] is different from our analytic expression by a term

$$\frac{6\hat{s}\hat{u}(ee_cg_s^2)^2}{\hat{t}(\hat{s} + \hat{u})^2}, \quad (9)$$

which is exactly the contribution of photoh-ghost scattering diagram (*i.e.* the contribution of the unphysical polarization states of the external gluons) and should be subtracted from Eq. (A1) of [35]. Here

$$\hat{s} = (q + g_1)^2, \quad \hat{t} = (q - P)^2, \quad \hat{u} = (g_1 - P)^2. \quad (10)$$

In appendix, we give explicit expressions of $\overline{\Sigma}|M(\gamma + g \rightarrow (c\bar{c})[^{2S+1}L_j^{(1;8)}] + g)|^2$ for J/ψ production.

Known the spin, color average-squared matrix elements of the hard subprocesses, in the NRQCD framework, we obtain the subcross sections. The color-singlet photon-gluon fusion contribution to $J/\psi + jet$ production is well known [33]:

$$\begin{aligned} & \frac{d\hat{\sigma}}{d\hat{t}}[\gamma + g \rightarrow (c\bar{c})[^3S_1^{(1)}] + g \rightarrow J/\psi + jet] \\ &= \frac{1}{16\pi\hat{s}^2} \overline{\Sigma}|M(\gamma + g \rightarrow (c\bar{c})[^3S_1^{(1)}] + g)|^2 \\ & \times \frac{1}{18m_c} \langle 0 | \mathcal{O}_1^{J/\psi} [^3S_1] | 0 \rangle. \end{aligned} \quad (11)$$

where $\langle 0 | \mathcal{O}_1^{J/\psi} [^3S_1] | 0 \rangle$ is the color-singlet matrix element which is related to the lepton decay width of J/ψ . The average-squared matrix element $\overline{\Sigma}|M(\gamma + g \rightarrow (c\bar{c})[^3S_1^{(8)}] + g)|^2$ can be obtained from $\overline{\Sigma}|M(\gamma + g \rightarrow (c\bar{c})[^3S_1^{(1)}] + g)|^2$ by taking into account of different color factor. The color-octet $(c\bar{c})[^3S_1^{(8)}]$ contribution is

$$\begin{aligned} & \frac{d\hat{\sigma}}{d\hat{t}}[\gamma + g \rightarrow (c\bar{c})[^3S_1^{(8)}] + g \rightarrow J/\psi + g] \\ &= \frac{1}{16\pi\hat{s}^2} \frac{15}{6} \overline{\Sigma}|M(\gamma + g \rightarrow (c\bar{c})[^3S_1^{(1)}] + g)|^2 \\ & \times \frac{1}{24m_c} \langle 0 | \mathcal{O}_8^{J/\psi} [^3S_1] | 0 \rangle. \end{aligned} \quad (12)$$

The color-octet $(c\bar{c})[^3S_0^{(8)}]$ and $(c\bar{c})[^3P_J^{(8)}]$ contributions are

$$\begin{aligned} & \frac{d\hat{\sigma}}{d\hat{t}}[\gamma + g \rightarrow (c\bar{c})[^1S_0^{(8)}] + g \rightarrow J/\psi + jet] \\ &= \frac{1}{16\pi\hat{s}^2} \overline{\Sigma}|M(\gamma + g \rightarrow (c\bar{c})[^1S_0^{(8)}] + g)|^2 \\ & \times \frac{1}{8m_c} \langle 0 | \mathcal{O}_8^{J/\psi} [^1S_0] | 0 \rangle, \end{aligned}$$

$$\begin{aligned}
& \frac{d\hat{\sigma}}{d\hat{t}}[\gamma + g \rightarrow (c\bar{c})[{}^3P_J^{(8)}] + g \rightarrow J/\psi + jet] \\
&= \frac{1}{16\pi\hat{s}^2} \sum_J \bar{\Sigma} |M(\gamma + g \rightarrow (c\bar{c})[{}^3P_J^{(8)}] + g)|^2 \\
&\times \frac{1}{8m_c} \langle 0 | \mathcal{O}_8^{J/\psi} [{}^3P_0] | 0 \rangle,
\end{aligned} \tag{13}$$

where the heavy quark spin symmetry

$$\langle 0 | \mathcal{O}_8^{J/\psi} [{}^3P_J] | 0 \rangle = (2J + 1) \langle 0 | \mathcal{O}_8^{J/\psi} [{}^3P_0] | 0 \rangle \tag{14}$$

is exploited.

C. The z and P_T distributions of J/ψ

Now we consider the z and P_T distribution of J/ψ produced in process Eq.(1). Based on the factorization theorem for the lepton induced hard diffractive hard scattering [13], the differential cross section can be expressed in terms of a diffractive parton distribution [14,15] as

$$\begin{aligned}
d\sigma &= \frac{df_{g/p}^{diff}(x_1, x_{\mathbb{P}}, t, \mu)}{dx_{\mathbb{P}} dt} dx_{\mathbb{P}} dt \cdot \\
&\frac{d\hat{\sigma}(\gamma + g \rightarrow J/\psi + jet)}{d\hat{t}} dx_1 d\hat{t}.
\end{aligned} \tag{15}$$

Here

$$\frac{df_{g/p}^{diff}(x_1, x_{\mathbb{P}}, t, \mu)}{dx_{\mathbb{P}} dt} dx_1 \tag{16}$$

represents the probability of finding in the proton a gluon carrying momentum fraction x_1 , while leaving the proton intact except for been diffractively scattered with the momentum transfer $(x_{\mathbb{P}}, t)$. $x_{\mathbb{P}}$ is the fractional momentum loss of the diffracted proton, *i.e.*, $x_{\mathbb{P}} \simeq (p_{1z} - p'_{1z})/p_z$, and t is the invariant momentum transfer for the diffracted proton, *i.e.*, $t = (p_1 - p'_1)^2$.

We now consider the kinematics. It is convenient to introduce the variable

$$z \equiv \frac{p_1 \cdot P}{p_1 \cdot q}. \tag{17}$$

In the proton rest frame $z = E_\psi/E_\gamma$. In terms of z and P_T (the transverse momentum of J/ψ), the Mandelstam variables and x_1 can be expressed as the following:

$$\begin{aligned}
\hat{s} &= \frac{P_T^2}{z(1-z)} + \frac{m_\psi^2}{z}, \\
\hat{t} &= -\frac{(1-z)m_\psi^2 + P_T^2}{z}, \\
\hat{u} &= -\frac{P_T^2}{1-z}, \\
x_1 &= \frac{\hat{s}}{s_{\gamma p}}.
\end{aligned} \tag{18}$$

Here, $s_{\gamma p} = (q + p)^2$. The double differential cross section is

$$\frac{d\sigma}{dzdP_T} = \int_{x_1}^{x_{\mathbb{P}\max}} dx_{\mathbb{P}} \int_{-1}^0 dt \frac{df_{g/p}^{diff}(x_1, x_{\mathbb{P}}, t, \mu)}{dx_{\mathbb{P}} dt} \cdot \frac{d\hat{\sigma}(\gamma + g \rightarrow J/\psi + jet)}{d\hat{t}} J\left(\frac{x_1 \hat{t}}{zP_T}\right), \quad (19)$$

where the Jacobian can obtain from Eq.(18),

$$J\left(\frac{x_1 \hat{t}}{zP_T}\right) = \frac{2P_T \hat{s}}{z(1-z)s_{\gamma p}}. \quad (20)$$

The allowed regions of z, P_T are given by

$$0 \leq P_T \leq \sqrt{(1-z)(zx_{\mathbb{P}\max}s_{\gamma p} - m_{\psi}^2)}, \\ z_{\min} \leq z \leq z_{\max}, \quad (21)$$

with

$$z_{\max} = \frac{1}{2x_{\mathbb{P}\max}s_{\gamma p}} \left[x_{\mathbb{P}\max}s_{\gamma p} + m_{\psi}^2 + \sqrt{(x_{\mathbb{P}\max}s_{\gamma p} - m_{\psi}^2)^2 - 4x_{\mathbb{P}\max}s_{\gamma p}P_T^2} \right], \\ z_{\min} = \frac{1}{2x_{\mathbb{P}\max}s_{\gamma p}} \left[x_{\mathbb{P}\max}s_{\gamma p} + m_{\psi}^2 - \sqrt{(x_{\mathbb{P}\max}s_{\gamma p} - m_{\psi}^2)^2 - 4x_{\mathbb{P}\max}s_{\gamma p}P_T^2} \right]. \quad (22)$$

In order to suppress the Reggon contributions, we set $x_{\mathbb{P}\max} = 0.05$ as usual.

III. NUMERICAL RESULTS AND DISCUSSIONS

For numerical predictions, we use $m_c = 1.5\text{GeV}$, $\Lambda_4 = 235\text{MeV}$, and set the factorization scale and the renormalization scale both equal to the transverse mass of J/ψ , *i.e.*, $\mu^2 = m_T^2 = (m_{\psi}^2 + P_T^2)$. For the color-octet matrix elements $\langle 0 | \mathcal{O}_8^{J/\psi} [{}^3S_1] | 0 \rangle$, $\langle 0 | \mathcal{O}_8^{J/\psi} [{}^1S_0] | 0 \rangle$ and $\langle 0 | \mathcal{O}_8^{J/\psi} [{}^3P_0] | 0 \rangle$ we use the values determined by Beneke and Krämer [28] from fitting the direct J/ψ production data at the Tevatron using GRV LO parton distribution functions [36],

$$\begin{aligned} \langle 0 | \mathcal{O}_8^{J/\psi} [{}^3S_1] | 0 \rangle &= 1.12 \times 10^{-2} \text{GeV}^3, \\ \langle 0 | \mathcal{O}_8^{J/\psi} [{}^1S_0] | 0 \rangle + \frac{3.5}{m_c^2} \langle 0 | \mathcal{O}_8^{J/\psi} [{}^3P_0] | 0 \rangle \\ &= 3.90 \times 10^{-2} \text{GeV}^3. \end{aligned} \quad (23)$$

Since the matrix elements $\langle 0 | \mathcal{O}_8^{J/\psi} [{}^1S_0] | 0 \rangle$ and $\langle 0 | \mathcal{O}_8^{J/\psi} [{}^3P_0] | 0 \rangle$ are not determined separately, we choose

$$\begin{aligned} \langle 0 | \mathcal{O}_8^{J/\psi} [{}^1S_0] | 0 \rangle &= 1.0 \times 10^{-2} \text{GeV}^3, \\ \langle 0 | \mathcal{O}_8^{J/\psi} [{}^3P_0] | 0 \rangle / m_c^2 &= 8.3 \times 10^{-3} \text{GeV}^3, \end{aligned} \quad (24)$$

allowed by Eq.(23), and in accordance with NRQCD power counting rule. The value of the color-singlet matrix element is taken to be $\langle 0 | \mathcal{O}_1^{J/\psi} [^3S_1] | 0 \rangle = 1.16 \text{GeV}^3$. The diffractive gluon distribution function

$$\frac{df_{g/p}^{diff}(x_1, x_{\mathbb{P}}, t, \mu)}{dx_{\mathbb{P}} dt} \quad (25)$$

at $\mu^2 = 4 \text{GeV}^2$ has been extracted from data on DDIS and on diffractive photoproduction of jets at HERA in [16],

$$\begin{aligned} & \frac{df_{g/p}^{diff}(x_1, x_{\mathbb{P}}, t, \mu^2 = 4 \text{GeV}^2)}{dx_{\mathbb{P}} dt} \\ &= \frac{9\beta_0^2}{4\pi^2} \left[\frac{4m_p^2 - 2.8t}{4m_p^2 - t} \left(\frac{1}{1 - t/0.7} \right)^2 \right] x_{\mathbb{P}}^{-2\alpha(t)} \cdot \\ & a_g(1 - x_1/x_{\mathbb{P}}), \end{aligned} \quad (26)$$

and is evolved in μ^2 according to the DGLAP evolution equations [13]. Here $\beta_0 = 1.8 \text{GeV}^{-1}$, $\alpha(t) = 1.14 + 0.25t$, $a_g = 4.5 \pm 0.5$. We use the central value of a_g for numerical calculation. In order to suppress the elastic J/ψ photoproduction (with or without proton dissociation) contribution and higher-twist corrections, a P_T cut $P_T \geq 1.0 \text{GeV}$ is imposed.

In Fig.3 we show the z distribution $\frac{d\sigma}{dz}$ of J/ψ produced in process Eq.(1) at HERA at a typical energy $\sqrt{s_{\gamma p}} = 100 \text{GeV}$ and with a P_T cut $P_T \geq 1.0 \text{GeV}$. The thin dash-dotted and short dashed lines represent the color-singlet cotribution and the sum of the color-singlet and color-octet contributions respectively. We observe that for $z > 0.3$ the color-singlet contribution is about order of 10^0nb , so this process can be studied at HERA with present integrated luminosity. For completeness, in Fig.3, we also show the z distribution of J/ψ inelastic production $\gamma + p \rightarrow J/\psi + jet + X$ in the same kinematic region (upper part), in this case, the thick solid and dotted lines curves are the sum of the color-singlet and color-octet contributions and the color-singlet contribution respectively. In both case, including the color-octet contribution, the z distribution is strongly enhanced in high z region due to the gluon propagator in the color-octet channel (Fig.2.(g)-(h)). In inelastic case, this behavior of rapid growing at high z does not agree with the HERA data [37,38].

In Fig.4, we show the P_T distribution $\frac{d\sigma}{dP_T}$ at HERA with $\sqrt{s_{\gamma p}} = 100 \text{GeV}$ and a z cut $z \leq 0.8$. The code for the curves are the same as Fig.3. We find that for $J/\psi + jet$ diffractive photoproduction in process Eq.(1) the color-octet contributions are larger than the color-singlet contribution for $P_T > 2.6 \text{GeV}$.

In Fig.5, we show the $J/\psi + jet$ diffractive photoproduction cross section as a function of $\sqrt{s_{\gamma p}}$ with the cut, $P_T \geq 1.0 \text{GeV}, z \leq 0.8$. We observe that in the energy region considered the color-singlet contribution is about order of 10^0nb , so this process can be studied at HERA with present integrated luminosity, and can give valuable insights in the color-octet mechanism for heavy quarkonia production.

Recently, it was pointed out that the cross section with an additional z cut, say, $z < 0.8$, *cannot* be reliably predicted in NRQCD [34,39], because the NRQCD expansion is singular at $z = 1$, only an average cross section over a sufficiently large region close to $z = 1$ can be predicted. The z distribution itself requires additional non-perturbative information in the form of so-called shape functions. These shape functions are also required to predict the P_T distributions with an additional upper z cut, say, $z < 0.8$, but not if z is integrated up to its kinematic maximum. So in Fig.6, we show the the P_T distribution $\frac{d\sigma}{dP_T}$ at HERA with

$\sqrt{s_{\gamma p}} = 100\text{GeV}$ and with z is integrated from its lower cut 0.2 to its kinematic maximum. The code for the curves are the same as Fig.4. We find that for $J/\psi + jet$ diffractive photoproduction in process Eq.(1), without the upper z cut, the color-octet contributions are dominated in the whole P_T region considered, which exceed the color-singlet contribution by almost an order of magnitude. In Fig.7, the $J/\psi + jet$ diffractive photoproduction cross section as a function of $\sqrt{s_{\gamma p}}$ with z is integrated from its lower cut 0.2 to its kinematic maximum is shown. We observe that in the energy region considered the color-singlet contribution is in the region $1.4\text{nb} < \sigma^{diff.}(singlet) < 2.4\text{nb}$, while including the color-octet contributions, the cross section increased by about an order of magnitude.

Experimentally, the nondiffractive and elastic (with or without proton dissociation) background to the diffractive J/ψ photoproduction we studied must be dropped out in order to obtain useful information about the heavy quarkonia production mechanism, this can be attained by performing the rapid gap analysis together with a large P_T cut, say, $P_T \geq 1.0\text{GeV}$. If statistics is not a limitation, it might be preferable to use cut $P_T \geq 2\text{GeV}$.

In conclusion, in this paper, We present a study of $J/\psi + jet$ diffractive production in the direct photon process at HERA based on the factorization theorem for lepton-induced hard diffractive scattering and the factorization formalism of the nonrelativistic QCD (NRQCD) for quarkonia production. Using the diffractive gluon distribution function extracted from HERA data on diffractive deep inelastic scattering and diffractive dijet photon production, we show that this process can be studied at HERA with present integrated luminosity, and can give valuable insights in the color-octet mechanism for heavy quarkonia production.

Acknowledgments

This work is supported in part by the National Natural Science Foundation of China, Doctoral Program Foundation of Institution of Higher Education of China and Hebei Province Natural Science Foundation, China.

REFERENCES

- [1] M. L. Perl, *High Energy Hadron Physics* (John Wiley & Sons, Inc., 1974).
- [2] P. D. B. Collins, *An Introduction to Regge Theory and High Energy Physics* (Cambridge University Press, Cambridge, England, 1977); K. Goulianos, Phys. Rep. **101**, 169 (1985).
- [3] UA8 Collaboration, A. Brandt *et al.*, Phys. Lett. B **297**, 417 (1992) ; R. Bonino *et al.*, *ibid.* **211**, 239 (1988).
- [4] ZEUS Collaboration, M. Derrick *et al.*, Phys. Lett. B **315**, 481 (1993); **332**, 228 (1994); H1 Collaboration, T. Ahmed *et al.*, Nucl. Phys. **B429**, 477 (1994).
- [5] ZEUS Collaboration, M. Derrick *et al.*, Z. Phys. C **68**, 569 (1995) ; Phys. Lett. B **356**, 129 (1995); J. Breitweg *et al.*, Eur. Phys. J. C **1**, 81 (1998); **5**, 41 (1998); **6**, 43 (1999).
- [6] H1 Collaboration, T. Ahmed *et al.*, Phys. Lett. B **348**, 681 (1995) ; C. Adloff *et al.*, Z. Phys. C **76**, 613 (1997); Phys. Lett. B **428**, 206 (1998); Eur. Phys. J. C **5**, 439 (1998); **6**, 421 (1999).
- [7] CDF Collaboration, F. Abe *et al.*, Phys. Rev. Lett. **78**, 2698 (1997).
- [8] CDF Collaboration, F. Abe *et al.*, Phys. Rev. Lett. **79**, 2636 (1997).
- [9] For a recent review, see D. M. Jansen, M. Albrow, and R. Brugnera, hep-ph/9905537; A. Hebecker, hep-ph/9905226; G. Ingelman, DESY 99-009; G. A. Alves, hep-ex/9905009; P. Newman, hep-ex/9901026; P. Marage, hep-ph/9810551; H. Jung, hep-ph/9809373; A. Goussiou *et al.*, hep-ph/9806485.
- [10] G. Ingelman and P.E. Schlein , Phys. Lett. B **152**, 256 (1985).
- [11] UA4 Collaboration, D. Bernard *et al.*, Phys. Lett. B **186**, 227 (1987); E710 Collaboration, N. A. Amos *et al.*, Phys. Lett. B **301**, 313 (1993); CDF Collaboration, F. Abe *et al.*, Phys. Rev. D **50**, 5535 (1994).
- [12] K. Goulianos , Phys. Lett. B **358**, 379 (1995); **363**, 268(E) (1995) ; K. Goulianos and J. Montanha, hep-ph/9805496.
- [13] J.C. Collins, Phys. Rev. D **57**, 3051 (1998).
- [14] Z. Kunszt and W. J. Stirling, in *the International workshop on Deep Inelastic Scattering and Related Phenomena (DIS 96)*, edited by G. Agostini and A. Negri (World Scientific, Singapore, 1997); hep-ph/9609245; F. Hautmann, Z. Kunszt, and D. E. Soper, Phys. Rev. Lett. **81**, 3333 (1998).
- [15] A. Berera and D. E. Soper, phys. Rev. D **50**, 4328 (1994); **53**, 6162 (1996).
- [16] L. Alvero, J.C. Collins, J. Terron, and J.J. Whitmore, Phys. Rev. D **59**, 074022 (1999).
- [17] H. Jung, D. Krücker, C. Greub, and D. Wyler, Z. Phys. C **60**, 721 (1993).
- [18] Chao-Hsi Chang, Nucl. Phys. **B172**, 425 (1980); E. L. Berger and D. Jones, Phys. Rev. D **23**, 1512 (1981); R. Baier and R. Rukel, Z. Phys. C **19** 251 (1983).
- [19] For a recent review, see E. Braaten, S. Fleming and T.C. Yuan, Annu. Rev. Nucl. Part. Sci. **46**, 197 (1996); E. Braaten, hep-ph/9702225; hep-ph/9810390; M. Beneke, hep-ph/9703429.
- [20] CDF Collaboration, F. Abe *et al.*, Phys. Rev. Lett. **79**, 572 (1997); *ibid.*, **79**, 578 (1997).
- [21] E. Braaten and T.C. Yuan, Phys. Rev. Lett. **71**, 1673 (1993).
- [22] E. Braaten, M.A. Doncheski, S. Fleming and M. Mangano, Phys. Lett. B **333**, 548 (1994); M. Cacciari and M. Greco, Phys. Rev. Lett. **73**, 1586 (1994); D.P. Roy and K. Sridhar, Phys. Lett. B **339**, 141 (1994).
- [23] G.T. Bodwin, E. Braaten and G.P. Lepage, Phys. Rev. D **46**, R1914 (1992); *ibid.* **46**, R3703 (1992).
- [24] E. Braaten and S. Fleming, Phys. Rev. Lett. **74**, 3327 (1995).
- [25] G.T. Bodwin, E. Braaten and G.P. Lepage, Phys. Rev. D **51**, 1125 (1995); *ibid.* **55**, 5853(E) (1997).

- [26] W.E. Caswell and G.P. Lepage, Phys. Lett. B **167**, 437 (1986).
- [27] P. Cho and A.K. Leibovich, Phys. Rev. D **53**, 150 (1996); *ibid.* **53**, 6203 (1996).
- [28] M. Beneke and M. Krämer, Phys. Rev. D **55**, R5269 (1997).
- [29] G.P. Lepage, L. Magnea, C. Nakhleh, U. Magnea and K. Hornbostel, Phys. Rev. D **46**, 4052 (1992).
- [30] J. F. Amundson, O. J. P. Eboli, E. M. Gregores, and F. Halzen, Phys. Lett. B **390**, 323 (1997) and references therein; O. J. P. Eboli, E. M. Gregores, and F. Halzen, hep-ph/9901387.
- [31] A. Edin, G. Ingelman, and J. Rathsmann, Phys. Rev. D **56**, 7317 (1997).
- [32] R. D. Field, *Applications of Perturbative QCD* (Addison-Wesley Publishing Company, Inc., 1989); G. Sterman *et al.*, *Handbook of perturbative QCD*, Rev. Mod. Phys. **67**, 157 (1995).
- [33] E. L. Berger and D. Jones, Phys. Rev. D **23**, 1512 (1981).
- [34] M. Beneke, M. Krämer, and M. Vanttinen, Phys. Rev. D **57**, 4258 (1998).
- [35] P. Ko, Jungil Lee and H.S. Song, Phys. Rev. D **54**, 4312 (1996).
- [36] M. Glück, E. Reya and A. Vogt, Z. Phys. C **67**, 433 (1995).
- [37] H1 Collaboration, S. Aid *et al.*, Nucl. Phys. B **472**, 3 (1996).
- [38] ZEUS Collaboration, J. Breitweg, *et al.*, Z. Phys. C **76**, 599 (1997).
- [39] M. Beneke, I. Z. Rothstein, and M. B. Wise, Phys. Lett. B **408**, 373 (1997).

APPENDIX: THE SPIN, COLOR AVERAGE-SQUARED MATRIX ELEMENTS

In this appendix, we give explicit expressions for the spin, color average-squared matrix elements of photon-gluon fusion subprocesses. The results are obtained using the symbolic manipulations with the aid of REDUCE package.

$$\begin{aligned} & \overline{\Sigma} |M(\gamma + g \rightarrow (c\bar{c})[{}^3S_1^{(1)}] + g)|^2 \\ &= \frac{64}{12} (e e_c g_s^2)^2 m_\psi^2 \frac{\hat{s}^2(\hat{t} + \hat{u})^2 + \hat{t}^2(\hat{s} + \hat{u})^2 + \hat{u}^2(\hat{s} + \hat{t})^2}{(\hat{t} + \hat{u})^2(\hat{s} + \hat{u})^2(\hat{u} + \hat{t})^2} \end{aligned} \quad (27)$$

$$\begin{aligned} & \overline{\Sigma} |M(\gamma + g \rightarrow (c\bar{c})[{}^3S_1^{(8)}] + g)|^2 \\ &= \frac{15}{6} \overline{\Sigma} |M(\gamma + g \rightarrow (c\bar{c})[{}^3S_1^{(1)}] + g)|^2 \end{aligned} \quad (28)$$

$$\begin{aligned} & \overline{\Sigma} |M(\gamma + g \rightarrow (c\bar{c})[{}^1S_0^{(8)}] + g)|^2 \\ &= \frac{24\hat{s}\hat{u}(e e_c g_s^2)^2}{\hat{t}(\hat{s} + \hat{t})^2(\hat{s} + \hat{u})^2(\hat{t} + \hat{u})^2} \times \\ & \quad (\hat{s}^4 + 2\hat{s}^3\hat{t} + 2\hat{s}^3\hat{u} + 3\hat{s}^2\hat{t}^2 + 6\hat{s}^2\hat{t}\hat{u} + 3\hat{s}^2\hat{u}^2 + 2\hat{s}\hat{t}^3 \\ & \quad + 6\hat{s}\hat{t}^2\hat{u} + 6\hat{s}\hat{t}\hat{u}^2 + 2\hat{s}\hat{u}^3 + \hat{t}^4 + 2\hat{t}^3\hat{u} + 3\hat{t}^2\hat{u}^2 + 2\hat{t}\hat{u}^3 + \hat{u}^4) \\ &= \frac{24\hat{s}\hat{u}(e e_c g_s^2)^2}{\hat{t}(\hat{s} + \hat{t})^2(\hat{s} + \hat{u})^2(\hat{t} + \hat{u})^2} \{[\hat{u}^2 + (\hat{s} + \hat{u} + \hat{t})(\hat{s} + \hat{t})]^2 - 2\hat{s}\hat{t}(\hat{s} + \hat{t})^2 + \hat{s}^2\hat{t}^2\} \end{aligned} \quad (29)$$

$$\begin{aligned} & \sum_J \overline{\Sigma} |M(\gamma + g \rightarrow (c\bar{c})[{}^3P_J^{(8)}] + g)|^2 \\ &= \frac{96(e e_c g_s^2)^2}{\hat{t} m_\psi^2 (\hat{s} + \hat{t})^3 (\hat{s} + \hat{u})^3 (\hat{t} + \hat{u})^3} \times \\ & \quad (7\hat{s}^7\hat{t}\hat{u} + 7\hat{s}^7\hat{u}^2 + 25\hat{s}^6\hat{t}^2\hat{u} + 38\hat{s}^6\hat{t}\hat{u}^2 + 21\hat{s}^6\hat{u}^3 + 2\hat{s}^5\hat{t}^4 + 47\hat{s}^5\hat{t}^3\hat{u} + 88\hat{s}^5\hat{t}^2\hat{u}^2 + 78\hat{s}^5\hat{t}\hat{u}^3 \\ & \quad + 35\hat{s}^5\hat{u}^4 + 4\hat{s}^4\hat{t}^5 + 63\hat{s}^4\hat{t}^4\hat{u} + 132\hat{s}^4\hat{t}^3\hat{u}^2 + 156\hat{s}^4\hat{t}^2\hat{u}^3 + 98\hat{s}^4\hat{t}\hat{u}^4 + 35\hat{s}^4\hat{u}^5 + 2\hat{s}^3\hat{t}^6 + 47\hat{s}^3\hat{t}^5\hat{u} \\ & \quad + 136\hat{s}^3\hat{t}^4\hat{u}^2 + 190\hat{s}^3\hat{t}^3\hat{u}^3 + 156\hat{s}^3\hat{t}^2\hat{u}^4 + 78\hat{s}^3\hat{t}\hat{u}^5 + 21\hat{s}^3\hat{u}^6 + 13\hat{s}^2\hat{t}^6\hat{u} + 70\hat{s}^2\hat{t}^5\hat{u}^2 + 136\hat{s}^2\hat{t}^4\hat{u}^3 \\ & \quad + 132\hat{s}^2\hat{t}^3\hat{u}^4 + 88\hat{s}^2\hat{t}^2\hat{u}^5 + 38\hat{s}^2\hat{t}\hat{u}^6 + 7\hat{s}^2\hat{u}^7 + 13\hat{s}\hat{t}^6\hat{u}^2 + 47\hat{s}\hat{t}^5\hat{u}^3 + 63\hat{s}\hat{t}^4\hat{u}^4 + 47\hat{s}\hat{t}^3\hat{u}^5 \\ & \quad + 25\hat{s}\hat{t}^2\hat{u}^6 + 7\hat{s}\hat{t}\hat{u}^7 + 2\hat{t}^6\hat{u}^3 + 4\hat{t}^5\hat{u}^4 + 2\hat{t}^4\hat{u}^5) \end{aligned} \quad (30)$$

FIGURES

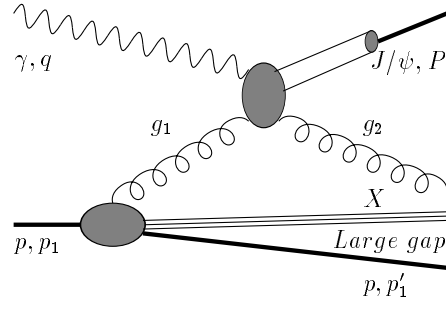


Fig.1. Sketch diagram for $J/\psi + jet$ diffractive production.

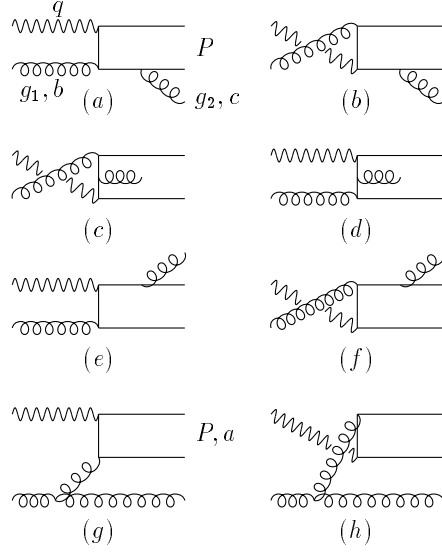


Fig.2. Feynman diagrams for $\gamma + g \rightarrow c\bar{c}[^{2S+1}L_J^{(1,8)}] + g$ subprocess. (a)-(f) contribute to color-singlet $c\bar{c}[^3S_1^{(1)}]$ and color-octet $c\bar{c}[^3S_1^{(1)}]$ production, (a)-(h) contribute to color-octet $c\bar{c}[^1S_0^{(8)}]$ and $c\bar{c}[^3P_J^{(8)}](J = 0, 1, 2)$ production.

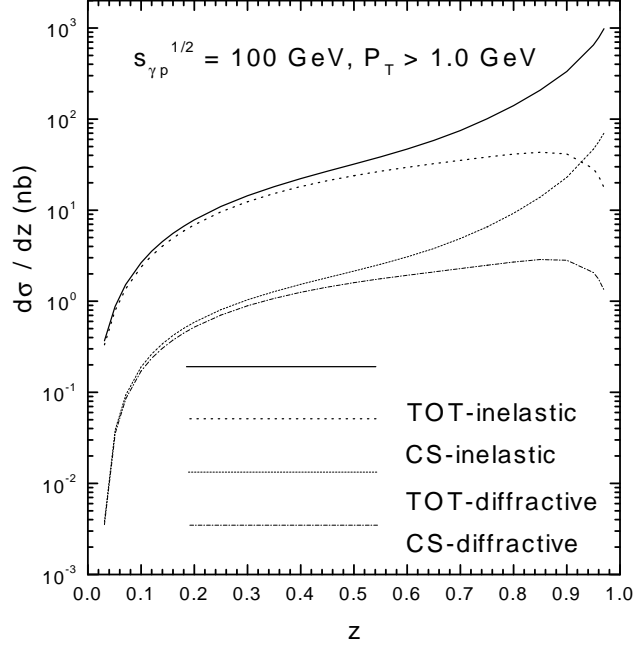


Fig.3. z distribution $d\sigma/dz$ for $J/\psi+jet$ production at HERA at $\sqrt{s_{\gamma p}} = 100\text{GeV}$, integrated over the J/ψ transverse momentum P_T with a lower P_T cut $P_T \geq 1.0\text{GeV}$. The thin dash-dotted and short dashed lines represent the color-singlet contribution and the sum of the color-singlet and color-octet contributions to $J/\psi+jet$ diffractive photoproduction $\gamma+p \rightarrow J/\psi+jet+p+X$ respectively. The thick solid and dotted lines curves are the sum of the color-singlet and color-octet contributions and the color-singlet contribution to inelastic $J/\psi+jet$ photoproduction $\gamma+p \rightarrow J/\psi+jet+X$ respectively.

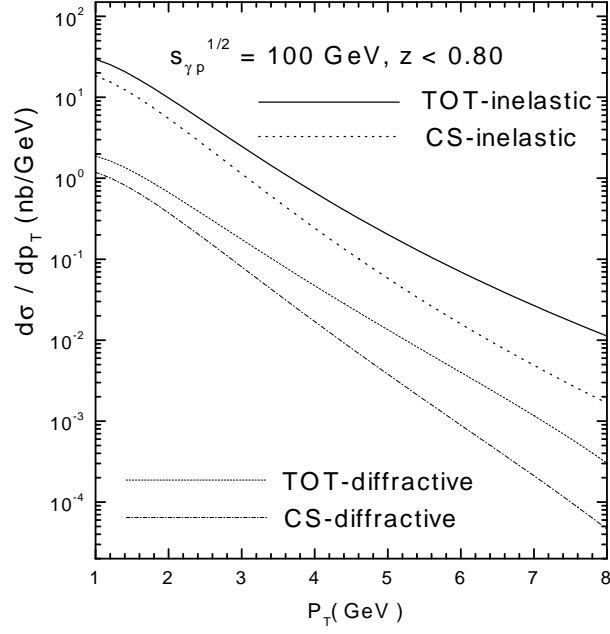


Fig.4. Transverse momentum (P_T) distribution $d\sigma/dP_T$ for $J/\psi + jet$ production at HERA at $\sqrt{s_{\gamma p}} = 100\text{GeV}$, integrated over z with a upper z cut $z \leq 0.8$. The thin dash-dotted and short dashed lines represent the color-singlet contribution and the sum of the color-singlet and color-octet contributions to $J/\psi + jet$ diffractive photoproduction $\gamma + p \rightarrow J/\psi + jet + p + X$ respectively. The thick solid and dotted lines curves are the sum of the color-singlet and color-octet contributions and the color-singlet contribution to inelastic $J/\psi + jet$ photoproduction $\gamma + p \rightarrow J/\psi + jet + X$ respectively.

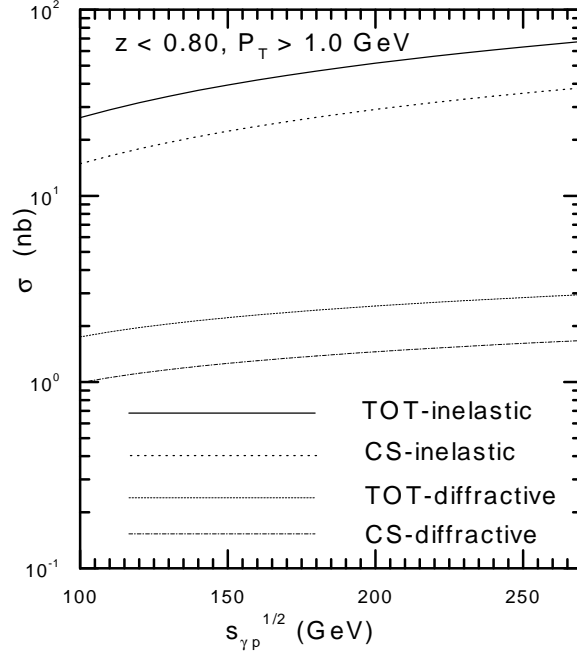


Fig.5. Total $J/\psi + jet$ photoproduction cross section for $P_T \geq 1.0 \text{ GeV}, z \leq 0.8$ as a function of $\sqrt{s_{\gamma p}}$. The thin dash-dotted and short dashed lines represent the color-singlet contribution and the sum of the color-singlet and color-octet contributions to $J/\psi + jet$ diffractive photoproduction $\gamma + p \rightarrow J/\psi + jet + p + X$ respectively. The thick solid and dotted lines curves are the sum of the color-singlet and color-octet contributions and the color-singlet contribution to inelastic $J/\psi + jet$ photoproduction $\gamma + p \rightarrow J/\psi + jet + X$ respectively.

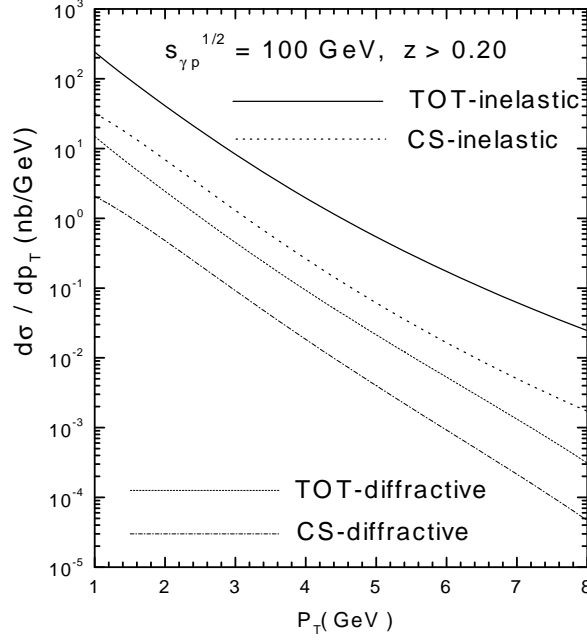


Fig.6. Transverse momentum (P_T) distribution $d\sigma/dP_T$ for $J/\psi + jet$ production at HERA at $\sqrt{s_{\gamma p}} = 100\text{GeV}$ with z is integrated from its lower cut 0.2 to its kinematic maximum. The thin dash-dotted and short dashed lines represent the color-singlet contribution and the sum of the color-singlet and color-octet contributions to $J/\psi + jet$ diffractive photoproduction $\gamma + p \rightarrow J/\psi + jet + p + X$ respectively. The thick solid and dotted lines curves are the sum of the color-singlet and color-octet contributions and the color-singlet contribution to inelastic $J/\psi + jet$ photoproduction $\gamma + p \rightarrow J/\psi + jet + X$ respectively.

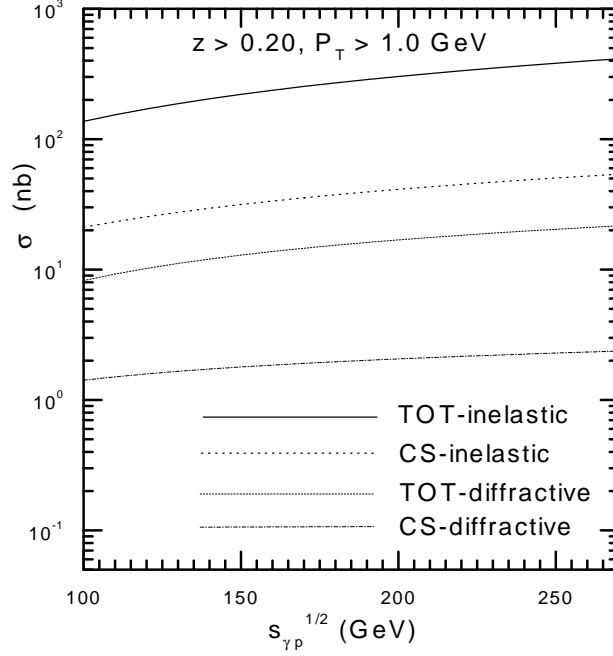


Fig.7. Total $J/\psi + jet$ photoproduction cross section for $P_T \geq 1.0\text{GeV}$, $z \geq 0.2$ as a function of $\sqrt{s_{\gamma p}}$. The thin dash-dotted and short dashed lines represent the color-singlet contribution and the sum of the color-singlet and color-octet contributions to $J/\psi + jet$ diffractive photoproduction $\gamma + p \rightarrow J/\psi + jet + p + X$ respectively. The thick solid and dotted lines curves are the sum of the color-singlet and color-octet contributions and the color-singlet contribution to inelastic $J/\psi + jet$ photoproduction $\gamma + p \rightarrow J/\psi + jet + X$ respectively.